The Laminin–Nidogen Complex is a Ligand for a Specific Splice Isoform of the Transmembrane Protein Tyrosine Phosphatase LAR

Pauline O'Grady, Tran Cam Thai, and Haruo Saito

Dana-Farber Cancer Institute and Department of Biological Chemistry and Molecular Pharmacology, Harvard Medical School, Boston, Massachusetts 02115

Abstract. Leukocyte antigen–related protein (LAR) is a prototype for a family of transmembrane protein tyrosine phosphatases whose extracellular domain is composed of three Ig and several fibronectin type III (FnIII) domains. Complex alternative splicing of the LAR-FnIII domains 4–8 has been observed. The extracellular matrix laminin–nidogen complex was identified as a ligand for the LAR-FnIII domain 5 (Fn5) using a series of GST-LAR-FnIII domain fusion proteins and testing them in in vitro ligand-binding assays. LAR–laminin–nidogen binding was regulated by alternative splicing of a small exon within the LAR-Fn5 so that inclusion of this exon sequence resulted in disruption of the laminin–nidogen-binding activity. Long cellular processes were observed when HeLa cells were plated on laminin–nidogen, but not when plated on a fibronectin surface. Indirect immunofluorescent antibody staining revealed high expression of LAR in a punctate pattern, throughout the length of these cellular processes observed on laminin–nidogen. Antibody-induced cross-linking of LAR inhibited formation of these cellular processes, and inhibition was correlated with changes in cellular actin cytoskeletal structure. Thus, LAR–laminin–nidogen binding may play a role in regulating cell signaling induced by laminin–nidogen, resulting in cell morphological changes.

REGULATION of protein tyrosine phosphorylation is a vital component of extracellular matrix (ECM)[1]–induced signal transduction. Changes in the tyrosine phosphorylation status of specific proteins are implicated in the cytoskeletal reorganization required for dynamic regulation of focal adhesion sites in signal transduction at these sites, and in the transmission of guidance signals in motile cells (2). Protein tyrosine phosphorylation is regulated by both protein tyrosine kinases and protein tyrosine phosphatases (PTPases; 12). Nevertheless, the role of PTPases in ECM-induced signal transduction is not well understood. A number of studies have implicated PTPase activity in cell adhesion, cell spreading, neurite extension, disassembly of focal adhesion sites, and in signal transduction at the tips of neuronal growth cones (2, 9, 11). However, with the exception of the transmembrane PTPase CD45, which

may regulate integrin-induced tyrosine phosphorylation in neutrophils (1), the identity and role of the transmembrane PTPase(s) involved have not been elucidated.

Leukocyte antigen–related protein (LAR) is a prototype for a family of transmembrane PTPases whose extracellular regions are composed of a combination of three Ig-like domains and several fibronectin-type III (FnIII) domains (see Fig. 1; 35, 37). Other members of this family include mammalian PTPδ and PTPσ, *Drosophila* DLAR, and chicken CRYP-α (24, 33, 43). LAR family PTPases are prime candidates for regulating ECM-induced signal transduction for the following reasons: the extracellular region of these PTPases has a close similarity with the neural cell adhesion molecule (N-CAM) family of cell-adhesion molecules (35); furthermore, LAR is located at the disassembly side of focal adhesion sites, and in cadherin-mediated cell–cell adhesion sites (18, 31). Chicken CRYP-α is localized to the tips of neuronal growth cones, and *Drosophila* homolog of human LAR (DLAR) plays a role in neuronal pathfinding (17, 33). Phenotypes of LAR knockout mice suggest that LAR may also play a role in morphogenesis of the mammary gland in mice (30).

The LAR cytoplasmic domain is composed of two PTPase domains, the second of which appears to be catalytically inactive (36). Physiological substrates for the LAR

---

1. *Abbreviations used in this paper*: CAM, cell adhesion molecule; ECM, extracellular matrix; EHS, Engelbreth-Holm-Swarm; FnIII, fibronectin type III domain; GST, glutathione S-transferase; HBS, Hepes buffered saline; LAR, leukocyte antigen–related protein; PTPase, protein tyrosine phosphatase.

PTPase are unknown. The LAR cytoplasmic domain binds to a coiled-coil protein LIP.1, which might link LAR to cytoskeletal structures (31). The LAR C-terminus also associates with a multidomain protein called Trio, which contains a protein kinase domain and two guanine nucleotide exchange factor domains that are, respectively, specific to Rac1 and RhoA (5). These observations indicate a potential role for LAR in cytoskeletal reorganization induced by cell–ECM contact that is mediated by Rac and Rho-like molecules (39).

A number of observations suggest that the extracellular domain of LAR also has an important function. The LAR extracellular domain is proteolytically cleaved and undergoes controlled shedding (31, 34). Furthermore, the FnIII domains are alternatively spliced in a tissue-specific and developmentally regulated manner (25, 42). The entire region containing the FnIII domains 4–7 is alternatively spliced out in PTPσ and PTPδ (24, 43). Although this form of alternative splicing has not been seen in LAR, we have previously demonstrated alternative splicing of the LAR FnIII domains 6 and 7, and of LAR FnIII domain 4 (25). We also reported the alternative splicing of a small exon (exon 13) within the LAR FnIII domain 5. Inclusion of exon 13 within FnIII domain 5 may have a particular function in neuronal tissue, since cells of neuronal origin express the highest amount of exon 13 containing mRNA. In all other cell types tested, the LAR isoform in which exon 13 is spliced out is the predominant form (25). Furthermore, alternative splicing of exon 13 is regulated in neuronal tissues during embryonic development (43). Perhaps more importantly, the alternatively spliced exon 13 is conserved among LAR-like PTPases (human LAR, rat LAR and PTPδ; 25, 28). These observations suggest that alternative expression of FnIII domains 4–7 may have a conserved function.

To study the role of the LAR FnIII domains 4–7, we constructed a series of GST-LAR FnIII domain fusion proteins and tested them in in vitro ligand-binding assays. Using this approach, the ECM laminin-nidogen complex was identified as a ligand for the LAR FnIII domain 5. The laminin–nidogen complex is a major component of the ECM that modulates cell adhesion, cell migration, neurite outgrowth, cell proliferation, and cell differentiation (21). The ability of laminin–nidogen to modulate such a wide range of events is related to its large size and multidomain structure that allows the interaction of laminin–nidogen with a number of different ligands. We found that alternative splicing of exon 13 within the LAR FnIII domain 5 regulated LAR–laminin-nidogen–binding activity. Furthermore, antibody-induced cross-linking of LAR in HeLa cells alters laminin-nidogen–induced cell morphology.

Materials and Methods

Cells

U373 MG (human glioblastoma) and HeLa (human epithelioid carcinoma) cells were obtained from the American Type Culture Collection (Rockville, MD). U373 MG were grown in Eagles media (GIBCO BRL, Gaithersburg, MD) containing 10% FCS. HeLa cells were grown in DME media (Bio-Whittaker, Walkersville, MD) containing 10% FCS and supplemented with 2 mM glutamine. Cells were maintained at 37°C in a humidified atmosphere with 10% CO_2.

Buffers

PBS: 10 mM sodium phosphate buffer (pH 7.4), 150 mM NaCl. HBS buffer: 10 mM Hepes (pH 7.4), 150 mM NaCl. SDS sample buffer: 0.125 M Tris (pH 6.8), 10% SDS, 25% glycerol, 0.01% bromophenol blue. Detachment buffer: 2 mM EDTA, PBS, 0.05% BSA. Wash media: serum-free DME media supplemented with 0.05% heat-inactivated BSA and 10 mM Hepes (pH 7.4). BSA was heat-inactivated at 80°C for 20 min.

Anti-LAR Monoclonal Antibodies

The anti-LAR monoclonal antibodies 75.3A, 11.1A, and 71.2E have been previously described (34). The anti-LAR monoclonal antibody 75.11.16 was raised by a similar approach using a GST-LAR Fn5-protein as antigen. The epitopes in the LAR extracellular domain recognized by these antibodies are as follows: mAb 75.3A, LAR Ig domain 1, 2, or 3; mAb 11.1A, between FnIII domain 8 and the transmembrane segment; mAb 71.2E, FnIII domain 6 or 7; mAb 75.11.16, LAR FnIII domain 5.

Other Antibodies

The antilaminin mAbs used were: antihuman laminin β1 chain (clone I) and antihuman laminin γ1 chain (clone II) from GIBCO BRL; and antihuman laminin (LAM-89) from Sigma Chemical Co. (St. Louis, MO). Affinity-purified rabbit polyclonal anti-Engelbreth-Holm-Swarm (EHS)-laminin was also from Sigma Chemical Co., and rabbit polyclonal anti-mouse laminin B1/B2 chain was from Upstate Biotechnology Inc. (Lake Placid, NY). Anti-human β2 microglobulin mAb MIG-B5 was from BioSource International (Camarillo, CA). Affini-pure rabbit anti–mouse IgG was from Jackson ImmunoResearch Laboratories, Inc. (West Grove, PA). Monoclonal anti-human integrin β1, anti-human talin, and anti-human vinculin antibodies were from Upstate Biotechnology Inc. HRP-conjugated rabbit anti–mouse IgG antibody and TRITC-conjugated goat anti–mouse IgG1 were from Southern Biotechnology Associates Inc. (Birmingham, AL).

Laminin and ECM Proteins

The following preparations of ECM proteins were used: Matrigel™ (basement membrane matrix from the mouse EHS sarcoma; Becton Dickinson, Bedford, MA); purified laminin–nidogen complex from the EHS sarcoma, and human fibronectin (Boehringer Mannheim, Indianapolis, IN).

GST–LAR–FnIII Fusion Proteins

Fusion proteins of glutathione S-transferase (GST) with various LAR FnIII domains were constructed using the *E. coli* expression vector pGEX-2T (Pharmacia Biotech. Inc., Piscataway, NJ; 32). The GST-fusion proteins used in this study are shown schematically in Fig. 1. Various segments of LAR cDNA with appropriate restriction sites for subcloning were generated by PCR and inserted in-frame into the pGEX-2T vector downstream of the GST coding sequence. Their nucleotide sequences were confirmed by DNA sequencing. Fusion protein synthesis was induced in exponentially growing *Escherichia coli* cultures by adding 0.1 mM isopropylthiogalactoside, and continued for 2 h at 25°C. Fusion proteins were extracted by solubilizing the bacterial pellet with 1% Triton X-100/PBS, containing 1.0 mM PMSF and 1.0 mM benzamidine for 30 min at room temperature, followed by sonication for 30 s at 4°C. Fusion proteins were affinity-purified using glutathione Sepharose beads. Beads were washed five times with PBS. The purity and sizes of the fusion proteins were confirmed by SDS-PAGE followed by Coomassie blue staining.

³⁵S-Labeling of Conditioned Media

U373 MG cells were grown to 80% confluency in 100-mm tissue culture dishes in Eagle's media containing 10% FCS. Cells were then washed twice with serum-free media and metabolically labeled with [^{35}S]methionine/cysteine (Dupont-NEN, Boston, MA). In brief, cells were incubated for 20 h in methionine-free media supplemented with [^{35}S]methionine/cysteine (80 μCi/ml), 5% dialyzed FCS (1,000 D cut-off), and 10 mM Hepes buffer (pH 7.4). Labeled media was collected at 4°C, the protease inhibitors (1.0 mM PMSF and 1.0 mM benzamidine) were added, and the media was centrifuged at 1,500 rpm in a Beckman J-6M/E centrifuge at 4°C.

Ligand-binding Assays

The different GST-LAR-fusion proteins (20 μg) bound to glutathione Sepharose beads were incubated with [^{35}S]methionine-labeled media (5 ml) collected from U373 MG cells. Incubation was carried out for 2 h at 4°C with rotation. The incubation was terminated by centrifuging the beads at 1,000 rpm in a Beckman J-6M/E centrifuge for 5 min at 4°C. The beads were washed four times with 5 ml of ice-cold HBS buffer. After the fourth wash, the beads were resuspended in SDS sample buffer, reduced with β-mercaptoethanol, boiled, and subjected to SDS-PAGE on a 5% gel. A sample of the media without incubation with the fusion proteins was run on the gel to assess the number and relative concentration of the labeled bands in the media. Gels were processed for autoradiography with En-hance™ (Dupont-NEN) according to the manufacturer's instructions. Dried gels were exposed to x-ray film in the presence of an enhancer screen.

Binding of GST-LAR Fn5 (with or without the exon 13 sequence) to Matrigel™ was assayed as follows. Glutathione bead–bound GST-LAR Fn5+ or Fn5− (20-μl beads coated with 40 μg protein) was diluted into 10 ml HBS containing 2 mM EDTA, 1.0 mM PMSF, and 1.0 mM benzami-dine, and mixed with various amount of Matrigel (150–750 μg) for 2 h at 4°C with rotation. The beads were then precipitated by centrifugation and washed four times with 5 ml of ice-cold HBS buffer each. After the final centrifugation, the beads were resuspended in SDS sample buffer, re-duced with β-mercaptoethanol, boiled, and subjected to SDS-PAGE on a 6.5% gel and immunoblotting. Blots were probed with the rabbit poly-clonal anti-mouse laminin B1/B2 chain antibody, followed by HRP-conju-gated goat anti–rabbit antibody. Bound antibodies were visualized by the enhanced chemiluminescence reagent (Amersham Life Science Inc., Ar-lington Heights, IL).

Binding of GST-LAR Fn5 proteins to the purified laminin-nidogen complex was assayed in a similar manner, except that the concentration of laminin-nidogen was kept constant (150 μg in 10 ml), while the amount of GST-LAR Fn5 protein bound to glutathione beads varied (50–150 μg of protein per 40 μl beads), and the mixtures were incubated for 3.5 h at 4°C with rotation. Samples were analyzed on a 5% SDS gel, and blots were probed with an affinity-purified polyclonal anti-laminin antibody.

Immunoblotting with Antilaminin Antibodies

Conditioned media collected from U373 MG cells was incubated with the GST-LAR fusion proteins as described in the binding assay above. Elec-trophoresis was carried out on a 3–12% gradient SDS-polyacrylamide gel under nonreducing conditions, or on a 5% SDS-polyacrylamide gel under reducing conditions. After electrophoresis, the gels were blotted to nitro-cellulose and probed with monoclonal antibodies specific to the laminin β$_1$ chain, laminin γ$_1$ chain, or laminin (LAM-89). Bound anti-laminin anti-bodies were detected with HRP-conjugated rabbit anti–mouse IgG anti-bodies and the enhanced chemiluminescence reagent. Purified laminin-1 was run in parallel in all the gels as a positive control.

LAR Cross-linking

HeLa cells at 30–50% confluency were detached by incubation in detach-ment buffer for 20 min at 37°C. Cells were washed three times at 4°C in wash media. Cells were resuspended in wash media at a concentration of 0.4×10^6 cells/ml, and 0.12×10^6 cells were plated per well on laminin–nidogen-coated 24-well tissue culture plates. Laminin–nidogen (Boeh-ringer Mannheim) was coated at a concentration of 20 μg/ml PBS over-night at 4°C. Before plating the cells, the laminin–nidogen-coated wells were blocked for 1 h at room temperature by incubation with 0.5% heat-inacti-vated BSA, and were then washed once with PBS. Cells were incubated for 1 h at 37°C to allow the cells to attach and begin to spread. Unattached cells were removed by washing with wash media at room temperature. The cells were then incubated with the anti-LAR mAb 75.3A, 75.11.16, or a control anti-human β2 microglobulin mAb, at a concentration of 20 μg/ml in wash media for 10 min at 37°C. A further control was the omission of a first antibody. The media containing the unbound antibodies was re-moved, and the bound antibodies were cross-linked with 60 μg/ml Affini-pure™ rabbit anti–mouse IgG. Incubation at 37°C was continued for a fur-ther 35 min. The cells were washed three times with PBS and fixed in 3.7% paraformaldehyde/PBS for 10 min at room temperature. The cells were washed four times with PBS and photographed by phase contrast mi-croscopy on a Axiovert 135 microscope (Carl Zeiss Inc., Thornwood, NY) using Tri-X400 film (Eastman Kodak Co., Rochester, NY). Fractions of

spread cells were quantified by counting at least four random fields for each of four separate experiments.

Immunofluorescent Microscopy

The laminin–nidogen complex (20 μg/ml) was coated overnight at 4°C onto sterile, acid-washed 12-mm glass coverslips (Fisher Scientific Co., Pittsburgh, PA) in 24-well dishes (Costar Corp., Cambridge, MA). HeLa cells were plated on the laminin–nidogen-coated coverslips, and were treated as described for the cross-linking assay above. Cell surface LAR was stained by a modification of the method of Serra-Pagès et al. (31). In brief, before LAR staining cells were fixed in 3.7% paraformaldehyde (Fisher Scientific Co.) in PBS for 10 min. Fixation was required before LAR staining in order to preserve the laminin–nidogen-induced cell mor-phology. For staining internalized LAR and other intracellular proteins (talin, vinculin, and actin), the cells were permeabilized with 0.4% Triton X-100 in PBS for 5 min after fixation. After four washes with PBS, non-specific binding sites were blocked with 10% goat serum in PBS (for LAR, talin, and vinculin stainings) or 1% BSA in PBS (for actin staining) for 30 min. LAR, talin, and vinculin were stained for 1 h with monoclonal anti-LAR (11.1A), anti-talin, and anti-vinculin antibodies (10 μg/ml), re-spectively, in PBS with 2% goat serum. After four washes with PBS, the bound antibodies were detected by incubation for 1 h with TRITC-conju-gated goat anti–mouse IgG$_1$ (at 1:100 dilution) in PBS with 2% goat se-rum. Actin was visualized by incubation of the cells with 2U rhodamine-conjugated phalloidin (Molecular Probes Inc., Eugene, OR) in blocking solution for 30 min according to the manufacturer's instructions. For all stainings, the specificity of staining was determined in control experiments in which either the primary antibody or both the primary and secondary antibodies were omitted.

After labeling, all slides were washed three times with PBS and mounted in Fluorsave (Calbiochem-Novabiochem Corp., La Jolla, CA). Slides were viewed on an Axiophot™ microscope (Carl Zeiss Inc.) equipped for epifluorescence. Photographs were taken on Tri-X400 black and white film (Eastman Kodak Co.).

Results

Ligand Binding of GST–LAR–FnIII Domain Fusion Proteins

The complex alternative splicing of FnIII domains 4–7 among LAR family members suggests that these domains may have an important function. One possibility is that this region of LAR encodes a ligand-binding site. To test this possibility, a series of GST fusion proteins containing various LAR-FnIII domains were constructed for testing in ligand-binding assays. The GST–LAR–FnIII constructs used in this study are shown schematically in Fig. 1 *b*. Most of the constructs that include the LAR-FnIII domain 5 were made in two different versions: with or without the alternatively spliced exon 13, which encodes nine amino acids. These versions are referred to as Fn5+ and Fn5− forms, respectively, throughout the text.

Initially we tested binding of the GST–LAR–FnIII fu-sion proteins to components of the conditioned media from cultured cells. Conditioned media is a potential source of ligands such as ECM proteins. Incubation of 20 μg GST–LAR–FnIII fusion proteins with [^{35}S]methionine-labeled conditioned media from U373 MG (human glio-blastoma) cells revealed specific binding of ∼350-, 220-, and ∼200-kD proteins to the GST-fusion constructs #3, #5, #7, and #8 (encoding Fn5−; Fn5−, 6, 7, 8; Fn3,4,5−; and Fn5−, 8, respectively; Fig. 2). The bound proteins are highly enriched by the LAR constructs when compared with their concentration in the original media. Specificity of binding is indicated by the observation that the ligand-binding constructs all contained the Fn5- domain. All of
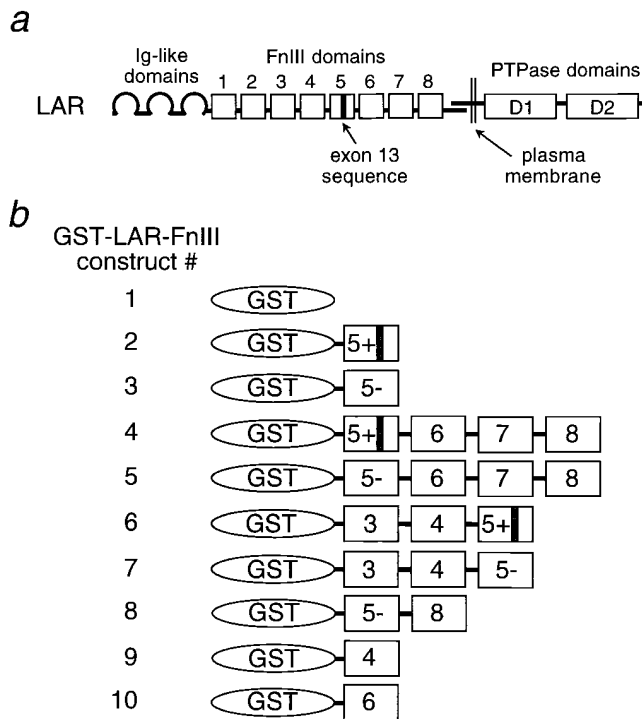
Figure 1. Schematic outline of GST-LAR-FnIII domain fusion proteins. The GST-LAR-fusion proteins constructed in the pGEX plasmid are shown (*b*). The numbered boxes represent the LAR-FnIII domains, and their position in the full-length LAR molecule is shown at the top (*a*). The presence or absence of the alternatively spliced exon in LAR-FnIII domain 5 is indicated by a + or − sign, respectively.
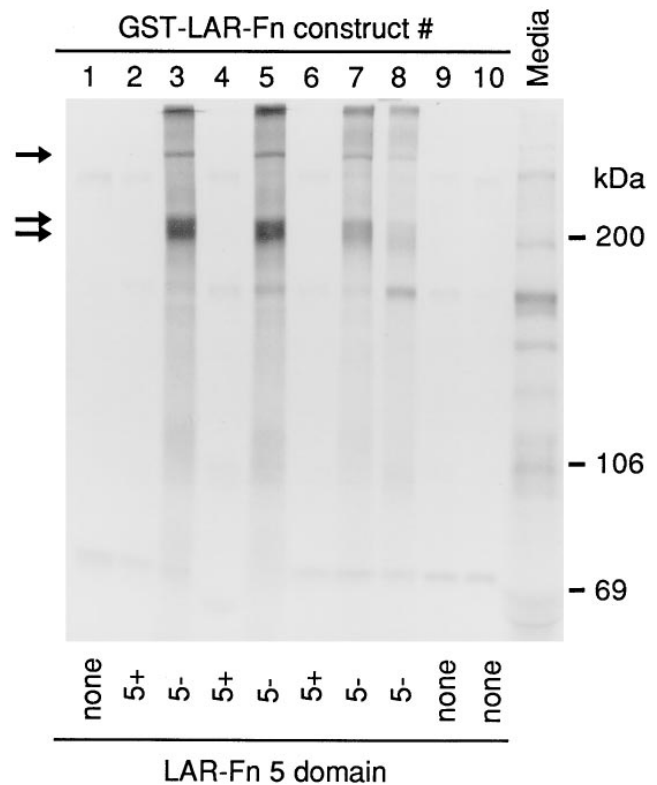

Figure 2. Ligand binding of GST-LAR-FnIII domain fusion proteins. The GST-LAR-FnIII domain fusion proteins, bound to glutathione beads, were incubated with [^{35}S]methionine-labeled conditioned media from U373 MG cells. The incubation was terminated by precipitation of the beads and associated proteins. After extensive washing, bound proteins were analyzed by 5% SDS-PAGE and autoradiography. The labeled bands of ∼350, 220, and 200 kD, which are specifically bound only by constructs encoding the LAR-FnIII domain 5-, are indicated by arrows. An aliquot of the labeled media, before incubation with the fusion proteins, is shown on the right (*Media*). Constructs are numbered as described in Fig. 1 *b*, and the presence of the 5+ or 5− domain is indicated at bottom.

the Fn5+-containing isoforms showed only background binding similar to the GST protein alone. The Fn5− isoform bound the same three labeled bands whether the Fn5− domain was present as a single domain (construct #3), or was flanked by other FnIII domains (constructs #5, #7, and #8). The binding was also independent of the distance from the Fn5− domain to the GST protein, indicating that the presence of the GST domain did not influence binding. Construct 8, in which Fn5− is joined directly to Fn8, shows a weaker binding than the other Fn5− constructs, suggesting that the presence of Fn6 and Fn7 may influence the ligand-binding activity of Fn5−. Fn4 or Fn6 alone do not show specific ligand binding (constructs #9 and #10). Thus, the Fn5− domain has a specific ligand-binding capacity, while inserting nine amino acids in this domain completely abolishes ligand binding.

The LAR-binding Protein Contains Laminin-1

The molecular masses of the Fn5−-binding proteins are similar to those of the ECM protein laminin-1. Laminin-1 is a disulfide-bonded heterotrimer of ∼350-, 220-, and ∼200-kD subunits (α_1, β_1, and γ_1 chains, respectively), and is reported to be synthesized and secreted into the media by U373 MG cells (19). Indeed, laminin chains immunoprecipitated from ^{35}S-labeled media of U373 MG cells migrated at the same positions as the Fn5- binding proteins (data not shown). We therefore tested if the Fn5−-binding protein is laminin by determining its reactivity to antilaminin antibodies.

First, the Fn5+ and Fn5− isoforms (constructs #2 and #3) were incubated with unlabeled conditioned media from U373 MG cells, and the bound proteins were separated by SDS-PAGE under nonreducing conditions followed by immunoblotting. Under nonreducing conditions, the laminin-1 trimer migrates as a protein of ∼850 kD. When probed with an antilaminin antibody, a high–molecular weight protein was detected bound to the Fn5−, but not to the Fn5+ isoform. This protein migrated at the same molecular weight as the purified laminin-1, which was run in parallel (Fig. 3 *a*). Next, the reactivity of antibodies specific to the laminin-β_1 and -γ_1 chains with the Fn5−-bound ligands was tested in a similar assay, except that electrophoresis was carried out under reducing conditions. The anti-β_1 and anti-γ_1 laminin antibodies detected bands of ∼220 kD and ∼200 kD, respectively, in the proteins bound to the Fn5−, but not to the Fn5+, isoform. These bands migrated at the same position as the laminin-β_1 and -γ_1 chains in purified laminin run in parallel (Fig. 3, *b* and *c*).

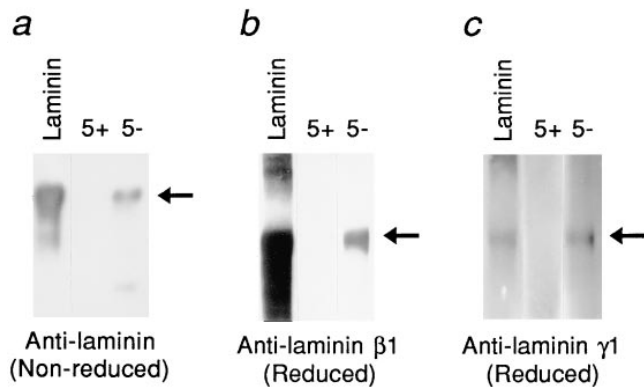Thus, laminin is specifically bound to the Fn5− fusion

Figure 3. Immunoblotting analysis of the GST–LAR–Fn5−-binding protein with anti-laminin antibodies. The identity of the GST-LAR-Fn5− ligand was tested by immunoblotting with anti-laminin antibodies. (a) GST-LAR-Fn5−-bound proteins were analyzed under nonreducing conditions on a 3–12% gradient SDS-polyacrylamide gel. Probing with the anti-laminin antibody recognizes a high molecular weight protein bound only by the GST-LAR-Fn5− (5−), but not by the GST–LAR–Fn5+ isoform (5+; *arrow at right*). This GST-LAR-Fn5− bound protein migrates at the same molecular weight as the purified laminin-1 trimer shown in lane 1. (b) and (c) GST-LAR-Fn5− bound proteins were analyzed under reducing conditions, which dissociate laminin-1 into its constituent α_1, β_1, and γ_1 chains. Blots were probed with the anti-laminin β_1 (b) or the anti-laminin γ_1 (c) antibodies. These antibodies detected proteins of $\sim$220 and 200 kD, respectively, which were bound by the GST-LAR-Fn5−, but not by the 5+ isoform (*arrows*). These bands migrated at an identical position to the β_1 and γ_1 chains in purified laminin-1 run in parallel (*laminin*).

protein. However, it cannot be concluded from these experiments alone whether laminin is bound directly to LAR, or indirectly via a molecule present in the conditioned media that acts as a bridge between laminin and LAR. Laminin-1 is generally found in a very tight 1:1 complex with the extracellular matrix protein nidogen (also known as entactin; 6, 40). The laminin–nidogen complex has binding sites for a number of different ligands, including collagen, perlecan, fibulin-1, heparin sulfate, and other ECM components (3, 27, 40). To examine if the Fn5− domain binds the laminin–nidogen complex directly or not, the Fn5− and 5+ isoforms were incubated with either Matrigel™ or the purified mouse laminin–nidogen complex. Matrigel™ is a preparation of ECM from the mouse EHS sarcoma, which is highly enriched for the laminin–nidogen complex (15). Incubation of the Fn5− and Fn5+ isoforms with increasing concentrations of Matrigel,™ followed by immunoblotting with an anti-laminin antibody, indicated a corresponding increase in binding of laminin to the Fn5−, but not the 5+ isoform (Fig. 4 *a*). In another experiment, the purified laminin–nidogen complex (constant amount) was incubated with increasing amounts of the Fn5− and Fn5+ proteins. The purified laminin–nidogen complex can also bind Fn5− in a dose-dependent manner, suggesting that LAR binding to the laminin–nidogen complex does not require any other ECM component (Fig. 4 *b*). At high concentrations of the Fn5+ protein, some laminin–nidogen binding is detected, suggesting that the Fn5+ may retain low-affinity binding to the laminin–nidogen complex. These data therefore indicate that the
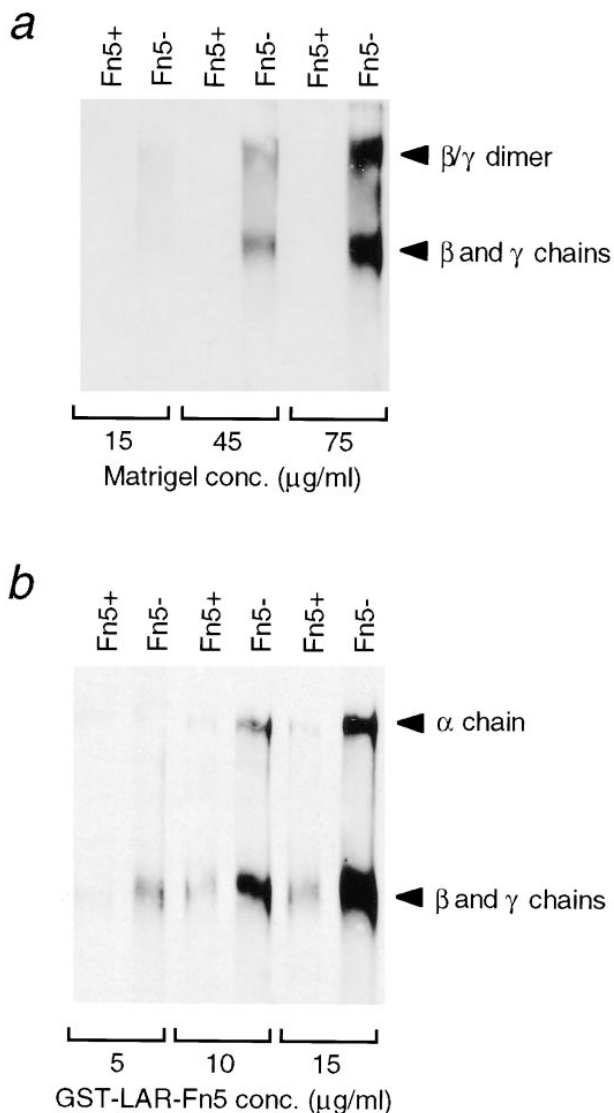

Figure 4. The laminin–nidogen complex directly binds the GST–LAR–FnIII domain 5- isoform in a dose-dependent manner. (a) The GST–LAR–Fn5− and Fn5+ isoforms (40 µg protein) bound to 20-µl glutathione beads were incubated with increasing concentrations of Matrigel™ (15–75 µg/ml in buffer; 10 ml total volume). Bead-bound proteins were analyzed by 6.5% SDS-PAGE and immunoblotting with a polyclonal anti-laminin $\beta_{1/\gamma1}$ chain antibody. (b) Increasing amounts of the GST–LAR–Fn5− and Fn5+ isoforms (50–150 µg protein) bound to 40 µl glutathione beads were incubated with the purified laminin–nidogen complex (15 µg/ml in buffer; 10 ml total volume). After extensive washing, bead-bound proteins were analyzed by 5% SDS-PAGE and immunoblotting with a polyclonal anti-laminin antibody. Positions of laminin subunits are indicated by arrows.

laminin–nidogen complex is a ligand for the LAR–Fn5− domain, although we cannot specify the exact binding site(s) on the laminin–nidogen complex.

Role of LAR–Laminin–Nidogen Binding in Cell Morphology

The above finding suggests a role for LAR in laminin–nidogen–mediated cellular events. Laminin–nidogen bind-
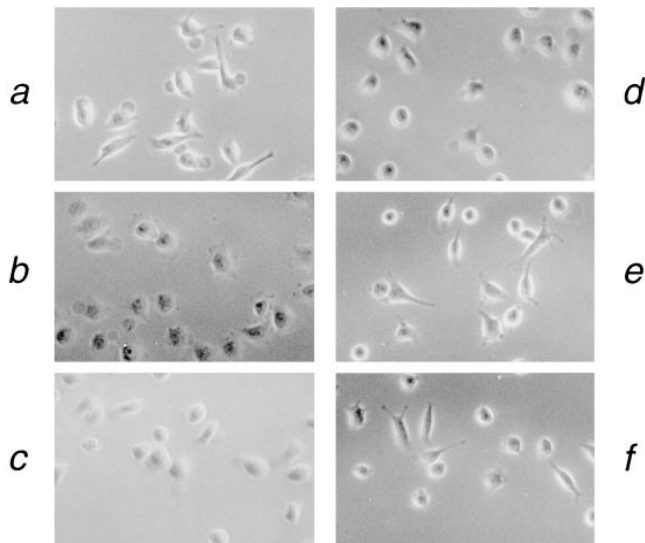
Figure 5. Effect of LAR cross-linking on HeLa cell morphology. HeLa cells were detached with EDTA and plated under serum-free conditions on the plates coated with the laminin–nidogen complex (*a, c–f*) or fibronectin (*b*) for 1 h at 37°C. LAR was then cross-linked by incubation for 10 min at 37°C with the anti-LAR mAbs 75.3A (*c*) or 75.11.16 (*d*), followed by a 35-min incubation with a rabbit anti–mouse IgG antibody. Controls in which HeLa cells were treated with no antibody (*a*); with the second antibody alone (*e*); or cross-linked with anti-β2 microglobulin antibody (*f*) are also shown. Cells were then fixed with 3.7% paraformaldehyde for 10 min at room temperature, and washed in PBS. The morphology of the cells was analyzed by phase contrast microscopy.

Table I. Effect of LAR Cross-linking on HeLa Cell Morphology

Cross-linking antibody	Fraction of spread cells with one or more long processes (%)			
	Expt. 1	Expt. 2	Expt. 3	Expt. 4
None	41.6% (331/795)	41.9% (131/313)	41.8% (76/182)	41.3% (57/138)
Anti-LAR (75.3A)	3.3% (21/630)	3.4% (6/176)	2.6% (5/190)	2.5% (2/81)
Anti-β2 microglobulin	41.7% (78/187)	36.7% (40/109)	53.8% (63/117)	

HeLa cells (1.2×10^5 cells/well) were plated on the laminin–nidogen complex. Antibody-induced cross-linking, cell fixation, and phase contrast microscopy were carried out as described in Fig. 5. In each experiment, fractions of spread cells with long extensions were quantified by counting cells from at least four randomly chosen fields. Expt., experiment.

ing to cells modulates a number of cellular activities, including cell differentiation, cell proliferation, cell adhesion, and cell motility (6, 21, 40). The localization of LAR to the disassembly side of focal adhesions suggests a role for LAR in regulation of focal adhesions (31). Since focal adhesions are sites of cell–ECM interaction and ECM-induced signal transduction, LAR could potentially regulate laminin–nidogen–mediated cell adhesion and motility.

The HeLa (human epithelioid carcinoma) cell line was chosen as a model system in which to investigate the functional role of laminin–LAR interaction, because HeLa cells express high amounts of the LAR protein that is predominantly the Fn5- isoform (25, 34). HeLa cells also exhibit a distinct morphology when plated on a laminin–nidogen substrate. After initial attachment and spreading on laminin–nidogen, long, thin cellular processes are extended from HeLa cells (Fig. 5 *a*). 95 min after plating, 42% of the spreading cells already exhibit long processes (Table I). These process are not observed when HeLa cells are attached to fibronectin (Fig. 5 *b*) or to the nonspecific attachment factor polylysine (data not shown). LAR cross-linking experiments were carried out to determine if LAR plays a role in the cell morphology induced by laminin–nidogen in HeLa cells. Antibody-induced cross-linking of LAR results in its aggregation on the cell surface, and ultimately its internalization (31; also see Fig. 6). Cross-linking of LAR in HeLa cells plated on a laminin–nidogen substrate caused a dramatic change in the morphology of the spreading cells. In LAR cross-linked cells, formation of the laminin–nidogen-induced cellular pro-

cesses is inhibited by 97%, although the cells do remain attached to the substrate (Table I; compare Fig. 5 *a* with Fig. 5, *c* and *d*). Similar inhibition of the cellular processes was observed using four different anti-LAR mAbs with distinct epitopes in the LAR extracellular domain (data not shown). Neither treatment of the cells with secondary antibody alone or a control cross-linking using anti-β2 microglobulin antibody affected the laminin–nidogen-induced cell morphology (Fig. 5, *e* and *f,* respectively). HeLa cells express surface β2 microglobulin (26), which has been shown to be sequestered after antibody-induced cross-linking (8).

Antibody-induced LAR cross-linking has been shown to induce patching and ultimately internalization of cell surface LAR (31). The extent of LAR internalization induced by cross-linking over the time period of our study was determined by immunofluorescence. Before LAR cross-linking, (after plating on laminin–nidogen for 1 h), a high concentration of cell surface LAR was visualized (Fig. 6 *a*.). After antibody-induced LAR cross-linking, however, cell surface LAR was barely detectable (Fig. 6 *b*). Permeabilization of the cross-linked cells followed by LAR staining revealed high concentrations of aggregated LAR within the cell, indicating internalization of LAR had occurred after cross-linking (Fig. 6 *c*). As a control, we examined localization of the integrin β_1 subunit after LAR cross-linking. The integrin β_1 subunit is a component of a number of integrin cell surface laminin receptors ($\alpha 1\beta_1$, $\alpha 2\beta_1$, $\alpha 3\beta_1$, $\alpha 6\beta_1$, and $\alpha 7\beta_1$). There were no significant changes in the distribution of the integrin β_1 subunit (data not shown), indicating that LAR cross-linking probably does not alter cell morphology through cointernalization of integrin laminin receptors.

Formation of cellular processes on laminin requires dynamic cytoskeletal reorganization. Actin staining of cells 1 h after plating on a laminin–nidogen substrate indicates a relatively disordered, meshwork actin cytoskeleton typical of spreading cells (Fig. 7 *a*). As the cell extends long processes, the actin skeleton becomes more organized, and a long, thick actin fiber is seen to extend from the cell body along the length of these processes (Fig. 7 *b*). This thick central actin fiber is absent from the LAR cross-linked cells where actin is present mainly as numerous thin stress fibers (Fig. 7, *c* and *d*). Thus, correlating with the effect on cell morphology, LAR cross-linking also affected the cellular cytoskeletal structure.

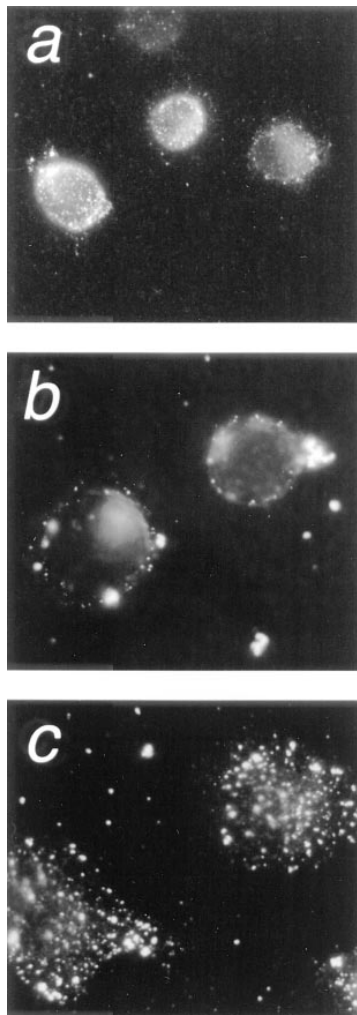Migration of cellular processes along an ECM requires

Figure 6. LAR cross-linking induces internalization of cell surface LAR. HeLa cells were plated on a laminin–nidogen substrate for 1 h (*a*), followed by LAR cross-linking with the anti-LAR mAb 75.3A (*b* and *c*) as described in the legend to Fig. 5. The cell surface LAR detected before LAR cross-linking (*a*) is almost abolished after antibody-induced LAR cross-linking (*b*). LAR staining of LAR cross-linked cells that have been permeabilized with 0.4% Triton X-100 reveal high concentrations of aggregated internalized LAR (*c*). Cells were fixed with 3.7% paraformaldehyde. LAR was stained with the anti-LAR mAb 11.1A and visualized by secondary staining with a TRITC-labeled anti-mouse antibody.

continuous assembly and disassembly of focal adhesions in order to provide traction during migration (13). Localization of LAR to the disassembly side of focal adhesions (31) suggests a mechanism by which LAR might influence the laminin-induced morphological changes in HeLa cells. To determine if LAR is localized to the cellular extensions, and thus might be involved in focal adhesion turnover, we visualized cellular localization of LAR as well as that of the focal adhesion–associated cytoskeletal proteins talin and vinculin, using immunofluorescence microscopy. LAR was highly enriched along the length of the cellular extensions, and was present in a punctate pattern (Fig. 8, *a* and *b*). Talin and vinculin were also present in these extensions, suggesting that focal adhesions are important for the
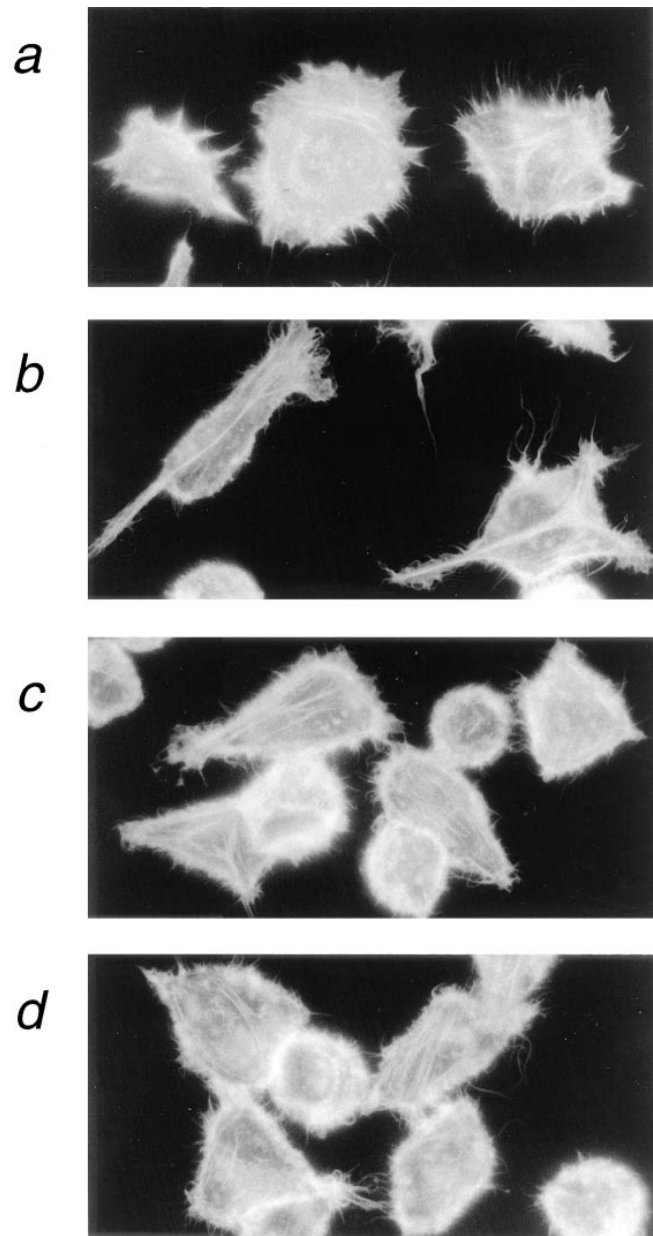

Figure 7. LAR cross-linking inhibits laminin-induced cytoskeletal reorganization in HeLa cells. HeLa cells were plated on a laminin–nidogen substrate, and LAR was cross-linked with the anti-LAR mAb 75.3A as described in the legend to Fig. 5. Cells were fixed with 3.7% paraformaldehyde, permeabilized with 0.4% Triton X-100, and stained for actin with rhodamine phalloidin. After initial cell attachment (1 h at 37°C), the actin cytoskeleton displays a meshwork structure (*a*). 45 min later, a linear actin spike is seen extended into the cellular process of control spreading cells (*b*). This actin spike is not observed in the LAR cross-linked cells (*c* and *d*).

formation or functioning of these cellular extensions (Fig. 8, *c* and *d*). Talin and vinculin are also abundant in the cell proper, where LAR was present in lower abundance. Predominant localization of LAR to the extended cell process suggests a specific role for LAR in this location. Antibody-induced internalization of LAR might inhibit formation of the cellular extensions by affecting the assembly–disassembly cycle of focal adhesion sites.
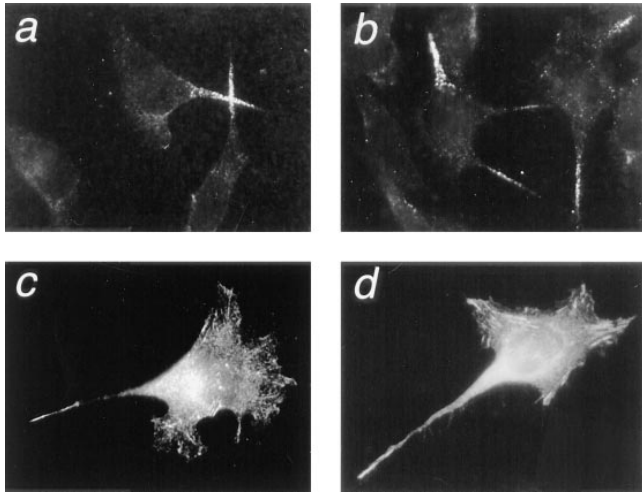
Figure 8. Indirect immunofluorescent staining of LAR (*a* and *b*), and the focal adhesion components talin (*c*) and vinculin (*d*) in HeLa cells spreading on a laminin–nidogen substrate. HeLa cells were plated on laminin for 1 h and 45 min as described in the legends to Fig. 5. Cells were fixed and stained for cell surface LAR with the anti-LAR mAb 11.1A as described in Fig. 6. Talin and vinculin were stained in cells that were permeabilized with 0.4% Triton X-100 after fixation. Stained proteins were visualized by secondary staining with a TRITC-labeled anti-mouse antibody.

Discussion

Elucidation of ligands for the extracellular domain of transmembrane PTPases is essential to understanding their physiological role in regulating signal transduction. Using GST fusion proteins representing LAR-FnIII domains in binding assays, we have shown that the ECM laminin–nidogen complex is a ligand for the LAR extracellular domain. The laminin–nidogen binding site was mapped to the LAR FnIII domain 5, and binding is regulated by alternative splicing of a small exon within this domain. We have further shown that LAR may play a role in regulating laminin–nidogen–induced cytoskeletal reorganization during cell spreading.

The extracellular domain of LAR is composed of a combination of Ig and FnIII domains similar to a number of cell adhesion molecules such as the N-CAM family. Two of these CAM-like molecules—NgCAM and the Deleted-in-Colorectal-Cancer protein—have been reported to bind laminin or a laminin-related protein netrin (10, 14). However, the laminin-binding region of these molecules has not been elucidated, and these molecules differ from LAR in that their cytoplasmic domains have no known direct signaling capabilities.

Based on the crystal structure of a FnIII domain of fibronectin (20), the amino acids encoded by the alternatively spliced exon 13 is in a surface-exposed loop region between β-pleated sheets. This position, together with the highly charged nature of the 9 amino acids encoded by exon 13 (WRPEESEDY), provides a potential mechanism for disrupting laminin–nidogen binding activity. Alternative splicing of exon 13 within the Fn5 domain is a conserved feature of the LAR family PTPases (25, 28). This result suggests that the FnIII domain 5 may function as a laminin–nidogen-binding site for all members of the LAR family.

We have previously shown that the FnIII domain 4, and FnIII domains 6 and 7, are also alternatively spliced. However, no specific ligands were found in our assays for the LAR-FnIII domains 6 and 7 or for the LAR-FnIII domain 4. It is possible that splicing of these FnIII domains functions in fine tuning the laminin–nidogen-binding properties of the FnIII domain 5. The lower laminin–nidogen-binding capacity of construct #8, in which Fn5 is directly linked to Fn8 without the intervening Fn6 and Fn7, lends support to this possibility (Fig. 2). Modulation of ligand binding of the RGD sequence of fibronectin by alternative splicing of a neighboring FnIII domain has been reported (22).

The relatively high level of expression of the non-laminin–nidogen binding LAR Fn5+ isoform in cells of neuronal origin, and upregulation of the LAR-Fn5+ isoform in confluent fibroblasts (25, 42) suggest that the LAR extracellular domain may have other ligands. Such ligand-binding activity may be mediated by the FnIII domains 1–3 or by the NH$_2$-terminal Ig domains of LAR. Ig domains of other cell surface proteins are often involved in homophilic and heterophilic interactions (29).

The LAR-Fn5− isoform is the predominant LAR isoform in most other cell types. Localization of both laminin–nidogen and LAR at focal adhesion sites is consistent with a role for the laminin–nidogen complex as an LAR ligand. However, assessment of the laminin–nidogen-binding capacity of cell surface–expressed LAR is complicated by coexpression of other laminin-binding cell surface molecules such as integrins, heparin sulfate, and β-1,4 galactosyltransferase (3, 27). Nevertheless, a role for LAR in modulating laminin-nidogen-induced cell morphological changes is indicated by the LAR antibody crosslinking studies (Fig. 5). The mechanism by which LAR cross-linking inhibits laminin–nidogen-induced cell spreading may be twofold. The first possibility is that laminin–nidogen-LAR binding and subsequent signaling is inhibited by antibody-mediated downregulation of LAR from the cell surface. LAR cross-linking does induce internalization of LAR over the time period used in our studies (31; Fig. 6). A second possibility is that antibody-induced LAR clustering may interfere with laminin–nidogen-induced LAR cellular localization, or may directly influence LAR PTPase activity, generating a signal antagonistic to laminin–nidogen-induced cell signaling. At the present time, our data cannot distinguish between these possible effects of LAR antibody cross-linking. Localization of both vinculin and talin to the cellular extensions, and high enrichment of LAR in these extensions (Fig. 8) suggest a role for LAR in modulating the assembly/disassembly of focal adhesion sites in these cellular extensions. This role for LAR would be consistent with the previous localization of LAR to the disassembly side of focal adhesions (31).

A crucial factor for regulating laminin-induced cell spreading is modulation of cell signaling through tyrosine phosphorylation (2). Definition of the role of the LAR PTPase activity requires elucidation of the physiological LAR substrate(s) as well as determination of the effect of laminin–nidogen–LAR binding on LAR PTPase activity. Few physiological substrates have been identified for any of the transmembrane PTPases. A number of potential LAR substrates, the tyrosine phosphorylation of which are implicated in cell spreading, are generated by laminin–

integrin interaction. These include the tyrosine kinases involved in reorganization of the actin cytoskeleton, signaling tyrosine kinases (FAK and Src), their downstream substrates such as the signaling molecule p130 CAS, and the cytoskeletal molecules tensin and paxillin (41).

There are a number of potential mechanisms (which are not mutually exclusive) by which laminin–nidogen binding to LAR may regulate LAR function. First, laminin–nidogen binding could induce clustering of LAR. Laminin-induced clustering of other cell surface ligands such as integrins, agrin, dystroglycan, and acetylcholine receptors has been well-documented, and integrin clustering is essential for FAK tyrosine kinase activation (4, 16, 38). Second, laminin–nidogen–LAR binding could change cellular localization of LAR, thus bringing it into the vicinity of its physiological substrates. Localization of other cell surface molecules is influenced by laminin binding (7, 23). The high enrichment of LAR and its punctate expression observed in the cellular processes formed by HeLa cells on a laminin–nidogen substrate is suggestive of this type of laminin-induced effect (Fig. 7). Third, since laminin–nidogen is a large molecular complex capable of simultaneously binding a number of ligands, laminin may cocluster LAR with other laminin ligands. Fourth, laminin–LAR binding may directly affect the LAR PTPase activity. At present, we cannot distinguish among these possibilities. Nonetheless, binding of laminin to a specific splice isoform of LAR may be the basis of a number of physiologically important events in which LAR (or LAR-family phosphatases) has been implicated, including cell migration, neuronal outgrowth, and mammary gland development (17, 30, 31). The role of LAR in laminin-induced cell morphological changes thus provides a focus for future studies to understand the mechanism by which the LAR PTPase coordinates laminin-induced cell signaling.

References

1. Arroyo, A.G., M.R. Campanero, P. Sánchez-Mateos, J.M. Zapata, M. Ursa, M. Angel del Pozo, and F. Sánchez-Madrid. 1994. Induction of tyrosine phosphorylation during ICAM-3 and LFA-1-mediated intercellular adhesion and its regulation by the CD45 tyrosine phosphatase. *J. Cell Biol.* 126:1277–1286.
2. Burridge, K., and M. Chrzanowska-Wodnicka. 1996. Focal adhesions, contractility, and signaling. *Annu. Rev. Cell Dev. Biol.* 12:463–519.
3. Castronovo, V. 1993. Laminin receptors and laminin-binding proteins during tumor invasion and metastasis. *Invasion Metastasis*. 13:1–30.
4. Cohen, M.W., C. Jacobson, P.D. Yurchenco, G.E. Morris, and S. Carbonetto. 1997. Laminin-induced clustering of dystroglycan on embryonic muscle cells: comparison with agrin-induced clustering. *J. Cell Biol.* 136:1047–1058.
5. Debant, A., C. Serra-Pagès, K. Seipel, S. O'Brien, M. Tang, and S.H. Park. 1996. The multidomain protein Trio binds the LAR transmembrane tyrosine phosphatase, contains a protein kinase domain, and has separate rac-specific and rho-specific guanine nucleotide exchange factor domains. *Proc. Nat. Acad. Sci. USA.* 93:5466–5471.
6. Dziadek, M. 1995. Role of laminin-nidogen complexes in basement membrane formation during embryonic development. *Experientia*. 51:901–913.
7. Eckstein, D.J., and B.D. Shur. 1992. Cell surface β-1,4-galactosyltransferase is associates with the detergent-insoluble cytoskeleton on migrating mesenchymal cells. *Exp. Cell Res*. 201:83–90.
8. Fujimoto, T. 1996. GPI-anchored proteins, glycosphingolipids, and sphingomyelin are sequestered to caveolae only after crosslinking. *J. Histochem. Cytochem*. 44:929–941.
9. Goldberg, D.J., and D.Y. Wu. 1996. Tyrosine phosphorylation and protrusive structures of the growth cone. *Perspect. Dev. Neurobiol.* 4:183–192.
10. Grumet, M., D.R. Friedlander, and G.M. Edelman. 1993. Evidence for the binding of Ng-CAM to laminin. *Cell Adhes. Comm.* 1:177–190.
11. Guan, J.-L., and H.-C. Chen. 1996. Signal transduction in cell-matrix interactions. *Int. Rev. Cytol.* 168:81–121.
12. Hunter, T. 1995. Protein kinases and phosphatases: the yin and yang of protein phosphorylation and signaling. *Cell.* 80:225–236.
13. Huttenlocher, A., R.R. Sandborg, and A.F. Horwitz. 1995. Adhesion in cell migration. *Curr. Opin. Cell Biol.* 7:697–706.
14. Keino-Masu, K., M. Masu, L. Hinck, E.D. Leonardo, S.S.-Y. Chan, J.G. Culotti, and M. Tessier-Lavigne. 1996. *Deleted in colorectal cancer (DCC)* encodes a netrin receptor. *Cell.* 87:175–185.
15. Kleinman, H.K., M.L. McGarvey, L.A. Liotta, P.G. Robey, K. Tryggvason, and G.R. Martin. 1982. Isolation and characterization of type IV procollagen, laminin and heparan sulfate proteoglycan from the EHS sarcoma. *Biochemistry*. 21:6188–6193.
16. Kornberg, L., E. Shelton, J.T. Parsons, M. Schaller, and R.L. Juliano. 1992. Cell adhesion or integrin clustering increases phosphorylation of a focal adhesion-associated tyrosine kinase. *J. Biol. Chem.* 267:23439–23442.
17. Krueger, N.X., D. Van Vactor, H.I. Wan, W.M. Gelbart, C.S. Goodman, and H. Saito. 1996. The transmembrane tyrosine phosphatase DLAR controls motor axon guidance in *Drosophila. Cell.* 84:611–622.
18. Kypta, R.M., H. Su, and L.F. Reichardt. 1996. Association between a transmembrane protein tyrosine phosphatase and the cadherin-catenin complex. *J. Cell Biol.* 134:1519–1529.
19. Mahesparan, R., B.B. Tysnes, K. Edvardsen, H.K. Haugeland, C.I.G., M. Lund-Johnsnen, O. Engebraaten, and R. Bjerkvig. 1997. Role of high molecular weight extracellular matrix proteins in glioma cell migration. *Neuropathol. Appl. Neurobiol.* 23:102–112.
20. Main, A.L., T.S. Harvey, M. Baron, J. Boyd, and I.D. Campbell. 1992. The three-dimensional structure of the tenth type-III module of fibronectin: an insight into RGD-mediated interactions. *Cell.* 71:671–678.
21. Malinda, K.M., and H.K. Kleinman. 1996. The laminins. *Int. J. Biochem. Cell Biol.* 28:957–959.
22. Manabe, R., N. Ohe, T. Maeda, T. Fukuda, and K. Sekiguchi. 1997. Modulation of cell-adhesive activity of fibronectin by the alternatively spliced EDA segment. *J. Cell Biol.* 139:295–307.
23. Miyamoto, S., S.K. Akiyama, and K.M. Yamada. 1995. Synergistic roles for receptor occupancy and aggregation in integrin transmembrane function. *Science*. 267:883–885.
24. Mizuno, K., K. Hasegawa, T. Katagiri, M. Ogimoto, T. Ichikawa, and H. Yakura. 1993. MPTPδ, a putative murine homolog of HPTPδ, is expressed in specialized regions of the brain and in the B-cell lineage. *Mol. Cell. Biol.* 13:5513–5523.
25. O'Grady, P., N.X. Krueger, M. Streuli, and H. Saito. 1994. Genomic organization of the human LAR protein tyrosine phosphatase gene and alternative splicing in the extracellular fibronectin type-III domains. *J. Biol. Chem.* 269:25193–25199.
26. Portillo, F., M. Pucciarelli, W. Jeffries, and B. Finlay. 1994. Salmonella typhimurium induces selective aggregation and internalization of host cell surface proteins during invasion of epithelial cells. *J. Cell Sci.* 107:2005–2020.
27. Powell, S.K., and H.K. Kleinman. 1997. Neuronal laminins and their cellular receptors. *Int. J. Biochem. Cell Biol.* 29:401–414.
28. Pulido, R., N.X. Krueger, C. Serra-Pagès, H. Saito, and M. Streuli. 1995. Molecular characterization of the human transmembrane protein tyrosine phosphatase δ: evidence for tissue-specific expression of alternative human transmembrane protein-tyrosine phosphatase δ isoforms. *J. Biol. Chem.* 270:6722–6728.
29. Ruoslahti, E., and B. Obrink. 1996. Common principles in cell adhesion. *Exp. Cell Res.* 227:1–11.
30. Schaapveld, R.Q., J.T. Schepens, G.W. Robinson, J. Attema, F.T. Oerlemans, J.A. Fransen, M. Streuli, B. Wieringa, L. Hennighausen, and W.J. Hendriks. 1997. Impaired mammary gland development and function in mice lacking LAR receptor-like tyrosine phosphatase activity. *Dev. Biol.* 188:134–146.
31. Serra-Pagès, C., N.L. Kedersha, L. Fazikas, Q. Medley, A. Debant, and M. Streuli. 1995. The LAR transmembrane protein tyrosine phosphatase and a coiled-coil LAR-interacting protein co-localize at focal adhesion. *EMBO (Eur. Mol. Biol. Organ.) J.* 14:2824–2838.
32. Smith, D.B., and K.S. Johnson. 1988. Single-step purification of polypeptides expressed in *Escherichia coli* as fusions with glutathione S-transferase. *Gene*. 67:31–40.
33. Stoker, A.W., B. Gehring, F. Haj, and B.-H. Bay. 1995. Axonal localization of the CAM-like tyrosine phosphatase CRYPα: a signaling molecule of embryonic growth cones. *Development*. 121:1833–1844.
34. Streuli, M., N.X. Krueger, P.D. Ariniello, M. Tang, J.M. Munro, W.A. Blattler, D.A. Adler, C.M. Disteche, and H. Saito. 1992. Expression of the receptor-linked protein tyrosine phosphatase LAR: proteolytic cleavage and shedding of the CAM-like extracellular region. *EMBO (Eur. Mol. Biol. Organ.) J.* 11:897–907.
35. Streuli, M., N.X. Krueger, L.R. Hall, S.F. Schlossman, and H. Saito. 1988.

A new member of the immunoglobulin superfamily that has a cytoplasmic region homologous to the leukocyte common antigen. *J. Exp. Med.* 168:1523–1530.

36. Streuli, M., N.X. Krueger, T. Thai, M. Tang, and H. Saito. 1990. Distinct functional roles of the two intracellular phosphatase like domains of the receptor-linked protein tyrosine phosphatases LCA and LAR. *EMBO (Eur. Mol. Biol. Organ.) J.* 9:2399–2407.

37. Streuli, M., N.X. Krueger, A.Y.M. Tsai, and H. Saito. 1989. A family of receptor-linked protein tyrosine phosphatases in humans and *Drosophila*. *Proc. Natl. Acad. Sci. USA*. 86:8698–8702.

38. Sugiyama, J.E., D.J. Glass, G.D. Yancopoulos, and Z.W. Hall. 1997. Laminin-induced acetylcholine receptor clustering: an alternative pathway. *J. Cell Biol.* 139:181–191.

39. Tapon, N., and A. Hall. 1997. Rho, Rac and Cdc42 GTPases regulate the organization of the actin cytoskeleton. *Curr. Opin. Cell Biol.* 9:86–92.

40. Timpl, R., M. Aumailley, M. Gerl, K. Mann, V. Nurcombe, D. Edgar, and R. Deutzmann. 1990. Structure and function of the laminin-nidogen complex. *Ann. NY Acad. Sci.* 580:311–323.

41. Yamada, K., and B. Geiger. 1997. Molecular interactions in cell adhesion complexes. *Curr. Opion. Cell Biol.* 9:76–85.

42. Zhang, J.S., and F.M. Longo. 1995. LAR tyrosine phosphatase receptor: alternative splicing is preferential to the nervous system, coordinated with cell growth and generates novel isoforms containing extensive CAG repeats. *J. Cell Biol.* 128:415–431.

43. Zhang, W.-R., N. Hashimoto, and B. Goldstein. 1993. PTP σ sequence. *GenBank Database*, www.ncbi.nlm.nih.gov. Accession No. L-11587.